Ablative Richtmyer-Meshkov and Rayleigh-Taylor instabilities in direct-drive laser fusion and growth reduction by adiabat shaping

A. Marocchino, S. Atzeni, A. Schiavi

Dipartimento SBAI, Università di Roma "La Sapienza" and CNISM, Italy

E-mail: alberto.marocchino@uniroma1.it

Abstract. One of the main design objectives for Inertial Confinement Fusion is the specification of surface roughness: surface perturbation triggers ablative instabilities that can cause shell rupture and/or hot-cold fuel mixing preventing the target from igniting. Understanding, controlling and measuring instabilities evolution is fundamental in order to design robust and efficient targets. The present work focuses on the ablative Rayleigh-Taylor instability (a-RTI); the a-RTI dispersion relation for high modes for a CH-DT-target [1] is presented and compared with a-RTI dispersion relation for an all-DT target [2]. The *Ablative region* and the *Blow-off region* are characterized via lagrangian line envelope graphs and isodensity line envelope graphs.

1. Introduction

Ignition target design for inertial confinement fusion (ICF) relies on accurate control of the asymmetry growth due to hydrodynamic instabilities such as the Rayleigh-Taylor instability (RTI) and the Richtmyer-Meshkov instability (RMI). Due to the extreme high temperatures both instabilities occur in their ablative form, e.g. a-RMI and a-RTI, where thermal conduction plays a key role and its effect is far away from being negligible [3, 4]. It has been shown by A. Marocchino et al. [5, 6] that for a thin shell target, e.g. the baseline HiPER target [2], irradiated by a direct drive scheme with a shaped laser pulse the two ablative instabilities are connected: the a-RMI evolves for the whole laser foot duration, while the a-RTI evolves during the laser plateau and it is triggered by the a-RMI (not completely damped). A key figure that summarizes the evolution for the two instabilities, and highlights the relation between the a-RMI and the a-RTI is fig. 2. In the limit of no adiabat shaping (case without initial picket) the a-RMI evolves until 7.5 ns, when its perturbation seeds the evolving and growing a-RTI. In the case with an adibat shaping picket the a-RMI, greatly reduced by the picket, evolves until 8.4 ns when the a-RTI is consequently seeded. This specific instability behaviour of two chained ablative instabilities holds in the limit of thin shell targets (refer to [5]) and ramped+plateau laser, fig. 1. The previous works [5, 6] refered to all-DT target, the present contribution focuses on the a-RTI for targets with a plastic ablator. Three

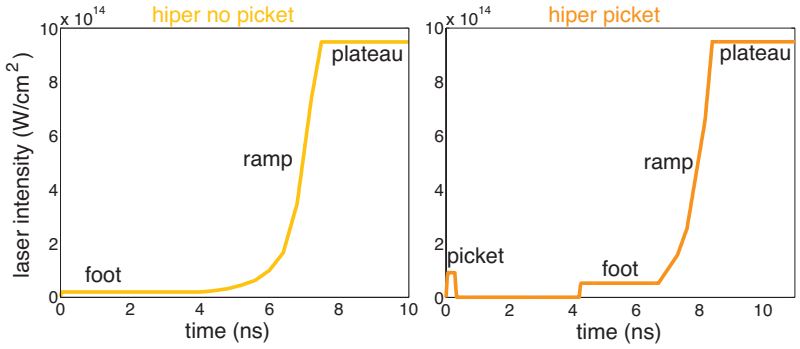

Figure 1. Laser profile schematic. Left image refers to the laser profile without adiabat shaping (no picket) for the HiPER baseline target; the right image refers to the laser profile with adiabat shaping (with picket) for the HiPER baseline target.

major results are discussed: an observation is about the a-RMI evolution regimes; the a-RTI dispersion relation for a target with plastic is obtained via 2D simulations and compared with the dispersion relation for the all-DT targets [2]; the blow-off and ablative regions described by V. Goncharov in [3] are characterized via lagrangian amplitude and isodensity amplitude line envelope graphs. Our first consideration concerns the a-RMI.

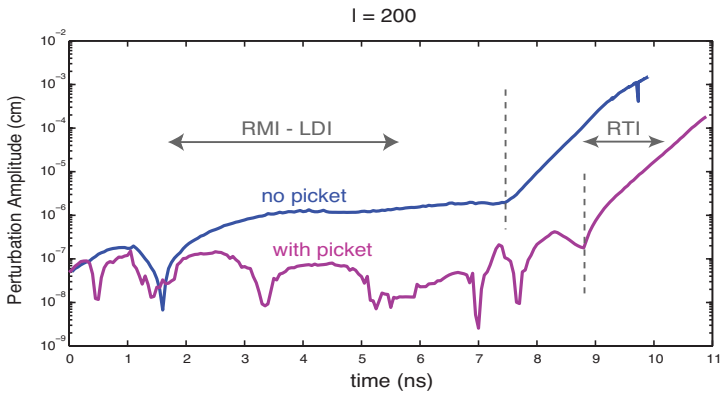

Figure 2. Instability amplitude evolution. A target with initial surface roughness exhibit an ablative RMI - Landau Darrieus Instability during the laser foot, the instability evolves in an a-RTI during the laser plateau.

The a-RMI occurring during the laser ramp, e.s. 0 ns - 7.5 ns for the no picket case, might be mixed with the Landau-Darrieus (LDI) instability: the a-RMI has a pure damping effect while the LDI tends to amplify the instability amplitude. We found possible to discriminate among three possible situations/regimes: a pure a-RMI regime, a pure LDI regime and a mixed regime. Saying k the wavenumber and D_c the distance between the critical density and the peak density, the following three regimes are distinguished:

$kD_c \gg 5$	ablative RMI
$1 < kD_c < 5$	ablative RMI + Landau Darrieus
$kD_c < 1$	Landau Darrieus

The above relation offers a straightforward physical interpretation, the a-RMI occurs only when the wavelength can be totally accommodated into the conduction length D_c.

2. Ablative Rayleigh-Taylor dispersion relation for CH-DT-target

In this section our interest is focused on the a-RTI instability; a CH-DT-target for direct drive is considered. The CH-DT-target originally proposed by G. Schurtz (see also [1]) is a cryogenic DT shell enclosed by 28 μm thick plastic shell, see fig. 3-right for target dimensions. Our interest is to study how fast the a-RTI grows and evolves, for this reason instability is only studied from 10.5 ns to 12.0 ns, i.e. a-RTI evolution interval. High l modes are considered: $50 < l < 950$, with $l = 2\pi R/\lambda$. Our simulations, fig. 3-left, have been performed both with no radiation and using multigroup flux-limited diffusive radiation model with LTE opacities. The case of no radiation is not physical, nevertheless these simulations are useful to understand the effect radiation transport has on the a-RTI. The a-RTI growth rate is analytically predicted by the Takabe-Betti formula [7]. Figure 3-left shows that a-RTI LTE radiation growth rates are about 66%

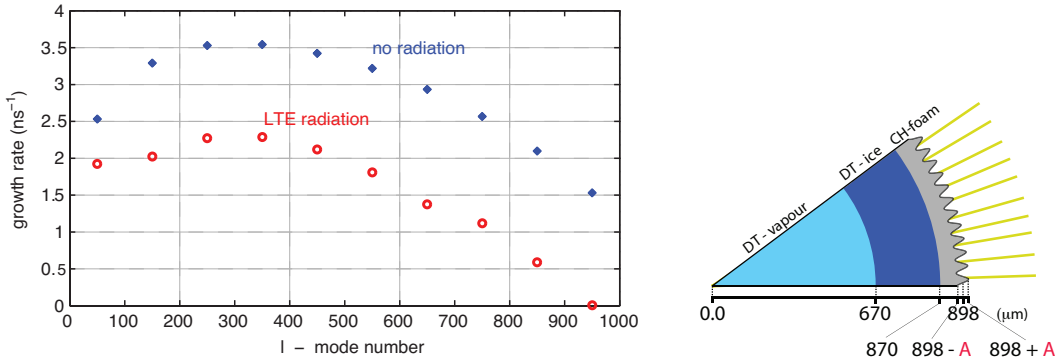

Figure 3. Left image: CH-DT-target a-RTI growth rates for the case with and without radiation. Right image: CH-DT-target dimensions.

of the equivalent case without radiation transport. Since energy is transported away from the perturbation, perturbed material is more compressed and consequently the instability expansion is slowed down; the growth rate is reduced. Radiation as expected plays a key role in optically thick material, such as foam folded target. In particular if the dispersion relation for the CH-DT-target is compared with the dispersion relation for the HiPER all-DT target [2, 5], we notice that the two targets are equivalently stable. The choice of a different target dimension (the CH-DT-target is smaller) and the different pulse shape allow to have significantly high ablation velocity (V_{abl}=2.15 μm/ns) compared to acceleration (g=64 μm/ns^2) so that the a-RTI growth rate also in the case of a target with plastic ablator is still limited.

3. Ablation region and Blow-off region

In RTI papers [3] the ablation front is subdivided into two regions: the *ablation* region and the *blow-off* region. The distinction arises from the different physics involved, in the ablation region thermal conduction plays a key role, while blow-off region is characterized as a plasma ballistically expanding. The ablation region spans from the peak density for a thermal conduction length $L = \frac{\gamma-1}{\gamma}\frac{kA}{\dot{m}}$, where γ is the ration of specific heat, A the average particle mass, $\dot{m}$ the mass ablation rate and k the Spitzer thermal conduction. Instabilities are theoretically predicted [3] to evolve in the ablation region and to ballistically expand in the blow off region. The ablation and blow-off regions are

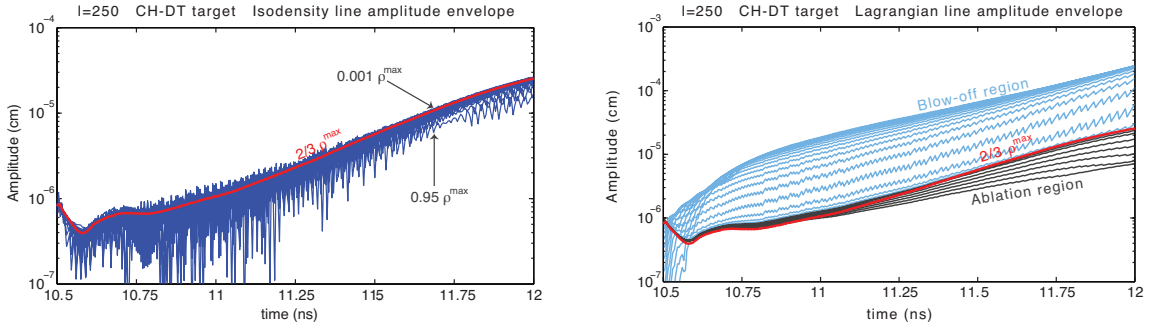

Figure 4. Line envelope grapths. Left image: isodensity line envelope. Isodensity lines are constantly accelerated and thus amplified up to 0.3-0.1$*\rho^{\max}$ where the amplitude stagnates. Right image: lagrangian line envelope, few lagrangian lines across the $2/3*\rho^{\max}$ are followed and their amplitude graphed: both the ablation region and the blow off region are easily spotted.

characterized via line envelope graphs: lagrangian line envelope graph and isodensity line envelope graph, refer to fig. 4. Figure 4-left is the isodentsity line amplitude envelope, where the $2/3*\rho^{\max}$ isodensity line is highlighted [5], the graph shows that the perturbation forming around the peak density ($\rho^{\max}$) grows for the whole ablation region reaching its maximum amplitude in the region that spans from $\sim 0.3\rho^{\max}$ to $\sim 0.1\rho^{\max}$. Figure 4-right is instead a lagrangian line amplitude envelope graph; the image shows how lagrangian lines expand up to approximately $2/3*\rho^{\max}$ and from that point on their undergo a ballistic expansion.

[1] Target proposed by G. Schurtz; for details see: S Atzeni, G Schurtz, Proc. of SPIE Vol. 8080 808022-1 (2011).
[2] S Atzeni, A Schiavi, C Bellei, Physics of Plasmas **14**(5) 052702 (2007).
[3] V N Goncharov et al., Physics of Plasmas **13**(1) 012702 (2006).
[4] S Atzeni, J Meyer-Ter-Vehn, Clarendon Press Oxford (2004).
[5] A Marocchino, S Atzeni, A Schiavi, Physics of Plasmas **17**(11) 112703 (2010).
[6] A Marocchino et al., 37th EPS Conf. Dublin, Ireland,21-25 June, 2010 **P4.223** (2010).
[7] R Betti, V N Goncharov, R L McCrory, C P Verdon, Physics of Plasmas **5**(5) 1446 (1998).
[8] S Atzeni, A Schiavi, A Marocchino, Plasma Physics and Controlled Fusion **53**(3) 035010 (2011).